NAIP proteins are required for cytosolic detection of specific bacterial ligands in vivo

Isabella Rauch,[1] Jeannette L. Tenthorey,[1] Randilea D. Nichols,[1] Khatoun Al Moussawi,[4] James J. Kang,[1] Chulho Kang,[3] Barbara I. Kazmierczak,[4,5] and Russell E. Vance[1,2,3]

[1]Division of Immunology and Pathogenesis, [2]Howard Hughes Medical Institute, and [3]Cancer Research Laboratory, University of California, Berkeley, Berkeley, CA 94720
[4]Department of Medicine and [5]Department of Microbial Pathogenesis, Yale University School of Medicine, New Haven, CT 06510

NLRs (nucleotide-binding domain [NBD] leucine-rich repeat [LRR]–containing proteins) exhibit diverse functions in innate and adaptive immunity. NAIPs (NLR family, apoptosis inhibitory proteins) are NLRs that appear to function as cytosolic immunoreceptors for specific bacterial proteins, including flagellin and the inner rod and needle proteins of bacterial type III secretion systems (T3SSs). Despite strong biochemical evidence implicating NAIPs in specific detection of bacterial ligands, genetic evidence has been lacking. Here we report the use of CRISPR/Cas9 to generate *Naip1*$^{-/-}$ and *Naip2*$^{-/-}$ mice, as well as *Naip1-6*$^{\Delta/\Delta}$ mice lacking all functional *Naip* genes. By challenging *Naip1*$^{-/-}$ or *Naip2*$^{-/-}$ mice with specific bacterial ligands in vivo, we demonstrate that *Naip1* is uniquely required to detect T3SS needle protein and *Naip2* is uniquely required to detect T3SS inner rod protein, but neither *Naip1* nor *Naip2* is required for detection of flagellin. Previously generated *Naip5*$^{-/-}$ mice retain some residual responsiveness to flagellin in vivo, whereas *Naip1-6*$^{\Delta/\Delta}$ mice fail to respond to cytosolic flagellin, consistent with previous biochemical data implicating NAIP6 in flagellin detection. Our results provide genetic evidence that specific NAIP proteins function to detect specific bacterial proteins in vivo.

NLRs (nucleotide-binding domain [NBD] leucine-rich repeat [LRR]–containing proteins) exhibit diverse functions in innate and adaptive immunity. Several NLRs form multiprotein cytosolic complexes called inflammasomes that recruit and activate caspase proteases, including CASPASE-1 (CASP1; Lamkanfi and Dixit, 2014). Active CASP1 induces an inflammatory form of cell death called pyroptosis and mediates the proteolytic cleavage and release of interleukins-1β and -18. Inflammasome activation in vivo also causes an "eicosanoid storm," a rapid release of signaling lipids resulting in pathological vascular leakage, increased hematocrit, and hypothermia (von Moltke et al., 2012). Together, diverse inflammasome-dependent responses help initiate innate immune responses against pathogens (von Moltke et al., 2013).

Several distinct inflammasomes have been described (von Moltke et al., 2013; Lamkanfi and Dixit, 2014), each responsive to distinct stimuli. NAIP (NLR family, apoptosis inhibitory protein)/NLRC4 (NLR family, caspase activation and recruitment domain [CARD] containing 4) inflammasomes are activated by the cytosolic presence of specific bacterial proteins. These include flagellin, as well as bacterial type III secretion system (T3SS) inner rod or needle proteins. C57BL/6 (B6) mice harbor four functional *Naip* genes (*Naip1*, *2*, *5*, and *6*) that are arranged in a cluster on chromosome 13 (Fig. 1 A). Interestingly, the *Naip* locus is variable between inbred mouse strains. For example, 129 mice additionally express *Naip4* and *Naip7*. Biochemical experiments suggest that individual NAIPs detect specific ligands. For example, in B6 mice, NAIP1 interacts with T3SS needle proteins (Zhao et al., 2011; Rayamajhi et al., 2013; Yang et al., 2013), NAIP2 interacts with T3SS inner rod proteins (Kofoed and Vance, 2011; Zhao et al., 2011; Suzuki et al., 2014; Tenthorey et al., 2014), and NAIP5 and NAIP6 interact with flagellin (Kofoed and Vance, 2011; Zhao et al., 2011; Tenthorey et al., 2014). Human NAIP recognizes T3SS needle and flagellin (Zhao et al., 2011; Yang et al., 2013; Kortmann et al., 2015). Upon engagement of their cognate ligands, NAIPs associate with NLRC4 to form a high-molecular-weight ring-shaped oligomer (Hu et al., 2015; Zhang et al., 2015). The assembled NAIP/NLRC4 inflammasome then recruits and activates CASP1 via the CARD in NLRC4.

Although NAIPs have been extensively characterized biochemically, genetic evidence they are essential for specific cytosolic detection of bacterial ligands is lacking. Classic genetic studies established a key role for *Naip5* in the innate response to *Legionella pneumophila* (Wright et al., 2003; Diez et al., 2003), a response later shown to require flagellin expression by *L. pneumophila* (Molofsky et al., 2006; Ren et al., 2006). The role of NAIP5 in detection of *L. pneu-*

Correspondence to Russell E. Vance: rvance@berkeley.edu

Abbreviations used: BMM, BM-derived macrophage; IRES, internal ribosome entry site; LDH, lactate dehydrogenase; NAIP, NLR family, apoptosis inhibitory protein; NLR, nucleotide-binding domain leucine-rich repeat–containing protein; PA, protective antigen; polyIC, polyinosinic:polycytidylic acid; sgRNA, single guide RNA; T3SS, type III secretion system.

The Rockefeller University Press $30.00
J. Exp. Med. 2016 Vol. 213 No. 5 657–665
www.jem.org/cgi/doi/10.1084/jem.20151809

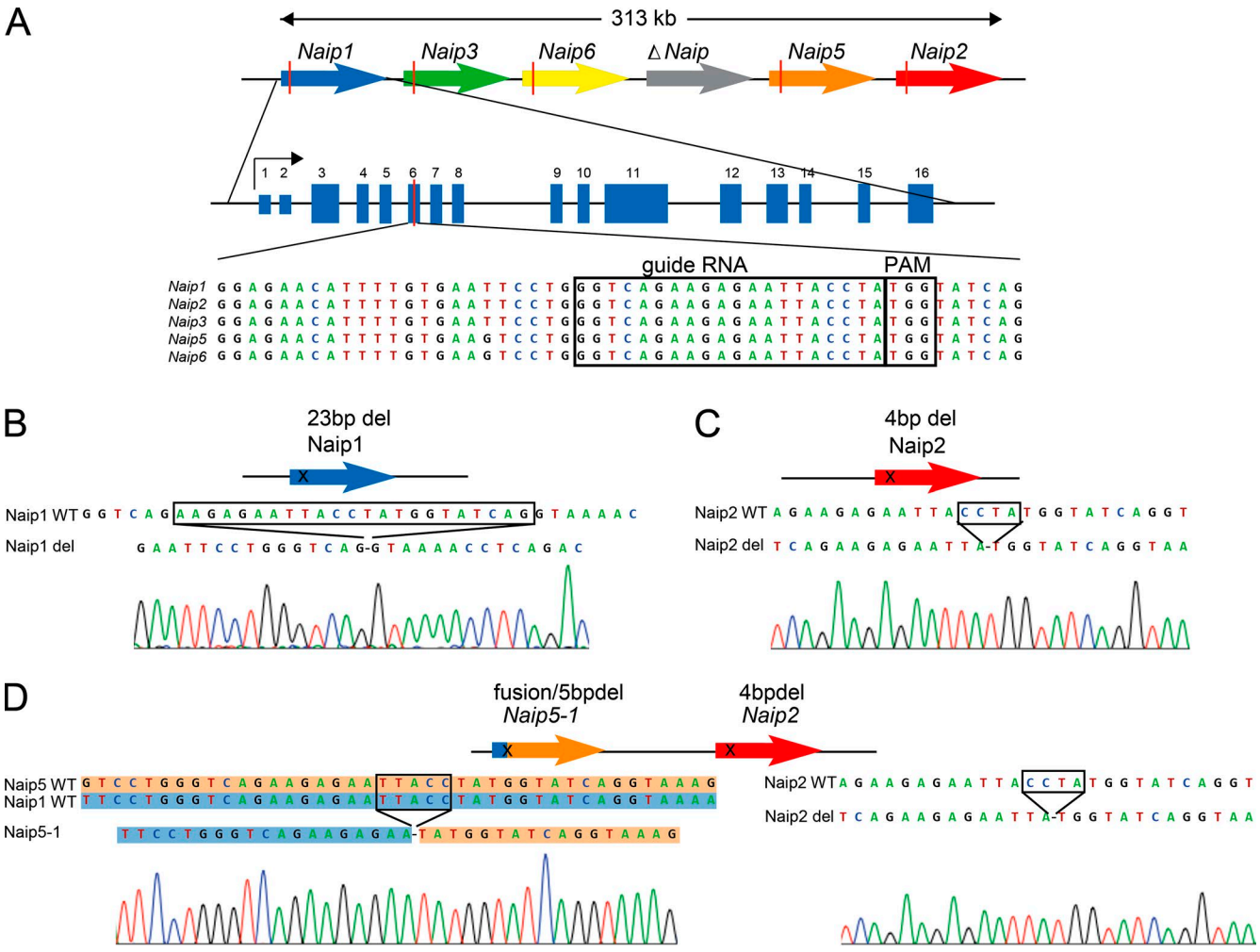

Figure 1. **CRISPR/Cas9 targeting strategy.** (A) *Naip* gene cluster in B6 mice. Guide RNA sequence for CRISPR/Cas9 targeting and protospacer-adjacent motif (PAM) are indicated. (B) The *Naip1* locus in WT and *Naip1*$^{-/-}$ mice. (C) The *Naip2* locus in WT and *Naip2*$^{-/-}$ mice. (D) The *Naip1* and *Naip5* loci in WT and *Naip1-6*$^{\Delta/\Delta}$ mice (left) and the *Naip2* locus in WT and *Naip1-6*$^{\Delta/\Delta}$ (right).

mophila was confirmed by the generation of *Naip5*$^{-/-}$ mice (Lightfield et al., 2008). However, *Naip5*$^{-/-}$ macrophages still undergo *Nlrc4*-dependent pyroptosis after transduction with flagellin (Lightfield et al., 2008) or infection with *Salmonella enterica* serovar Typhimurium (*S.* Typhimurium), presumably because of functional compensation by other *Naip* family members (Kofoed and Vance, 2011; Sellin et al., 2014). In addition, *Naip5*$^{-/-}$ mice show a partial inflammasome response to FlaTox, a toxin fusion that delivers flagellin systemically into the cytosol (von Moltke et al., 2012). To date, no other individual *Naip* gene has been disrupted by gene targeting, possibly because of the repetitiveness of the *Naip* locus. Mice lacking the entire *Naip* locus were recently reported (Sellin et al., 2014; Allam et al., 2015) and demonstrated the essentiality of *Naip* genes in the NLRC4 inflammasome response to *S.* Typhimurium. However, the requirement of specific *Naip* genes in the response to specific bacterial ligands remains unclear.

Recently, genome engineering of mice using the CRISPR/Cas9 endonuclease from *Streptococcus pyogenes* has been described (Wang et al., 2013). As Cas9 is targeted to genomic loci via a short ∼20-nucleotide sequence present in an associated guide RNA, Cas9 is ideally suited for genomic engineering of highly repetitive loci such as the *Naip* gene cluster. Here we describe our use of CRISPR/Cas9 to generate mice specifically lacking *Naip1*, *Naip2*, or all functional *Naips*. By challenging these mice with specific bacterial ligands, we provide genetic proof for the specificity and essentiality of NAIP proteins for the detection of cytosolic flagellin, T3SS needle, and T3SS rod proteins in vivo.

RESULTS AND DISCUSSION

Generation of *Naip*-deficient mice using CRISPR/Cas9

We designed a single guide RNA (sgRNA) that targets Cas9 to a 20-nucleotide sequence in exon 6 (the fourth coding exon) of all four functional *Naip* genes (*Naip1*, *2*, *5*, and *6*) in the

C57BL/6J genome (Fig. 1 A). This sequence is also present in *Naip3*. However, a cDNA for *Naip3* has not been characterized (Growney and Dietrich, 2000), and thus, *Naip3* is considered a pseudogene in the current mouse genome assembly (GRCm38; annotation release 105). The guide RNA sequence was not present in *delta-Naip*, which is truncated and believed to be nonfunctional. Cas9-targeted founder mice were screened for *Naip* mutations by PCR and sequencing of exon 6, and pure homozygous *Naip* mutant lines were then established.

The *Naip1*$^{-/-}$ line contains a 23-bp frameshift deletion in *Naip1* (Fig. 1 B), whereas the *Naip2*$^{-/-}$ line contains a 4-bp frameshift deletion in *Naip2* (Fig. 1 C). These deletions are predicted to result in NAIP proteins truncated before the NBD, a domain essential for NAIP function (Kofoed and Vance, 2011). No other *Naip* mutations were detected in these mouse lines. We failed to obtain mouse lines with specific modifications in only *Naip5* or *Naip6*. However, we did obtain mice lacking all functional *Naip* genes. In these *Naip1-6*$^{\Delta/\Delta}$ mice, *Naip2* was inactivated by a 4-bp frameshift deletion, whereas the sequence between *Naip5* exon 6 and *Naip1* exon 6 (including the entire *Naip6*, *Naip3*, and *delta-Naip* genes) was deleted, leading to a nonfunctional fusion of *Naip5* and *Naip1* (Fig. 1 D). Thus, we used a single Cas9/sgRNA complex to generate three different *Naip* mutant mouse lines.

Response of *Naip*-deficient macrophages to specific bacterial ligands

To determine whether *Naips* are required for inflammasome responses to specific bacterial ligands, we used a previously described retroviral lethality assay (Lightfield et al., 2008). In this assay, BM-derived macrophages (BMMs) are transduced with a retroviral construct encoding a specific NAIP ligand (flagellin, rod, or needle) upstream of an internal ribosome entry site (IRES)–GFP reporter. As representative ligands, we used retroviruses encoding flagellin (FlaA) from *L. pneumophila*, the T3SS inner rod (PrgJ) from *S.* Typhimurium, and the T3SS needle (BTH_RS04290) from *Burkholderia thailandensis*. WT BMMs transduced with these constructs activate the NAIP/NLRC4 inflammasome and undergo pyroptosis, resulting in few GFP^{+} cells. As a control, transduced *Nlrc4*$^{-/-}$ cells fail to undergo pyroptosis and thus express bacterial ligands and GFP. This assay permits analysis of responses to individual bacterial ligands independent of other ligands or confounding stimuli present during bacterial infections.

As previously reported, most WT BMMs transduced with T3SS needle protein undergo pyroptosis, despite low expression of *Naip1* in unprimed BMMs (Rayamajhi et al., 2013), whereas *Nlrc4*$^{-/-}$ cells are protected (Fig. 2, A and B). BMMs from *Naip1*$^{-/-}$ and *Naip1-6*$^{\Delta/\Delta}$ mice were also protected from needle-induced pyroptosis, whereas *Naip2*$^{-/-}$ and *Naip5*$^{-/-}$ cells were susceptible (Fig. 2, A and B). Conversely, *Naip2*$^{-/-}$ BMMs were protected from rod-induced pyroptosis but were susceptible to needle-induced pyroptosis (Fig. 2, A and B). Both *Naip1*$^{-/-}$ and *Naip2*$^{-/-}$ were fully susceptible to flagellin-induced pyroptosis. Flagellin-expressing retrovirus was consistently less efficiently transduced into cells than needle- or rod-retrovirus, likely because of the larger size of the flagellin protein. Only *Nlrc4*$^{-/-}$ and *Naip1-6*$^{\Delta/\Delta}$ BMMs were protected from all ligands, with *Naip1-6*$^{\Delta/\Delta}$ cells recapitulating the full protection observed in *Nlrc4*$^{-/-}$ cells (Fig. 2, A and B). These results demonstrate that endogenous NAIP proteins are essential for NLRC4-dependent pyroptosis in response to bacterial rod, needle, and flagellin proteins and, in addition, demonstrate that NAIP1 and NAIP2 are specifically required for NLRC4 activation in response to T3SS needle and rod, respectively.

Response of *Naip*-deficient macrophages to bacterial infection

To examine the role of *Naip* genes in pathogen detection, we infected BMMs with three bacterial pathogens known to activate the NLRC4 inflammasome and assessed pyroptosis-dependent release of intracellular lactate dehydrogenase (LDH). First we infected BMMs with a WT *S.* Typhimurium strain (LT2) encoding stimulatory T3SS rod and needle proteins and two flagellin proteins, FliC and FljB. Consistent with a previous study using an independent *Naip1-6*$^{\Delta/\Delta}$ mouse line (Allam et al., 2015), BMMs from our *Naip1-6*$^{\Delta/\Delta}$ mice showed reduced levels of cell death, equivalent to *Nlrc4*$^{-/-}$ BMMs. In contrast, *Naip1*$^{-/-}$ and *Naip2*$^{-/-}$ macrophages released amounts of LDH comparable with WT. *Naip5*$^{-/-}$ cells showed a slight, but statistically significant, protection from *S.* Typhimurium–induced pyroptosis (Fig. 3 A). These results suggest there is redundancy among various NAIPs for detection of *S.* Typhimurium. To simplify the repertoire of NAIP-stimulatory ligands expressed by *S.* Typhimurium, we used a *fliC/fljB* mutant strain that lacks flagellin expression. This strain induces overall lower levels of pyroptosis, possibly because of its reduced motility or infectivity or because recognition of flagellin (via NAIP5/6) contributes more significantly to pyroptosis than recognition of rod or needle. Nevertheless, *Naip2*$^{-/-}$ BMMs showed significantly reduced cell death in response to the *fliC/fljB* mutant strain, as compared with infected WT BMMs (Fig. 3 A), whereas loss of the flagellin sensor *Naip5* had no effect, as expected. If BMMs are prestimulated with polyinosinic :polycytidylic acid (polyIC) to induce *Naip1* expression (as previously reported [Rayamajhi et al., 2013]), *Naip1*$^{-/-}$ BMMs show a slight, but significant reduction in cell death as compared with WT BMMs. These data indicate that multiple NAIPs participate in NLRC4 activation by *S.* Typhimurium.

We next infected BMMs with *L. pneumophila*, a flagellated pathogen that encodes a type 4 secretion system but lacks a T3SS and thus inner rod and needle expression. As reported previously, *Nlrc4*$^{-/-}$ and *Naip5*$^{-/-}$ macrophages are protected from cell death upon *L. pneumophila* infection (Fig. 3 B; Lightfield et al., 2011). The lack of redundancy with NAIP6 in this experiment (as compared with results in Fig. 2) is most likely because lower levels of flagellin released during bacterial infection, as compared with retroviral trans-

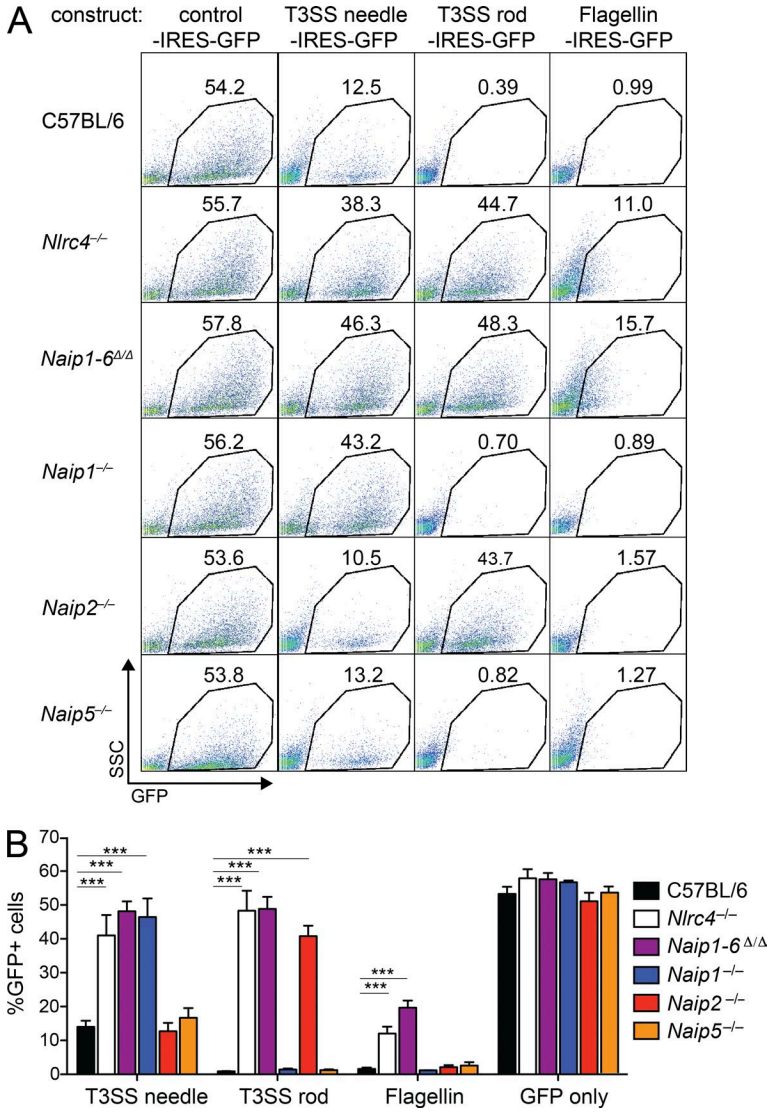

Figure 2. **Response of BMMs from WT and mutant mice to retrovirally transduced bacterial ligands.** (A) Representative flow plots of WT, *Nlrc4*$^{-/-}$, *Naip1-6*$^{\Delta/\Delta}$, *Naip1*$^{-/-}$, *Naip2*$^{-/-}$, and *Naip5*$^{-/-}$ BMMs transduced with control vector (IRES-GFP only) or with vectors encoding needle-IRES-GFP, inner rod-IRES-GFP or flagellin-IRES-GFP. Gates show the percentage of GFP-positive cells. (B) Quantification of retroviral transduction experiments. Data are representative of two independent experiments (n = 3), mean ± SD; one-way ANOVA, Dunnett's post test: ***, P < 0.001.

duction, increase the sensitivity to loss of *Naip5*. *Naip1-6*$^{\Delta/\Delta}$ BMMs are also protected from *L. pneumophila*–induced pyroptosis, whereas *Naip1*$^{-/-}$ and *Naip2*$^{-/-}$ cells release equal amounts of LDH as WT. Upon infection with an aflagellate strain of *L. pneumophila* (Δ*flaA*), no *Naip/Nlrc4*-dependent cell death could be observed, confirming flagellin is the only NAIP ligand in this pathogen. Plating of infected cell lysates for CFU showed that the decreased cell death in *S.* Typhimurium– or *L. pneumophila*–infected *Naip*- or *Nlrc4*-deficient cells was not caused by decreased intracellular replication of pathogens (not depicted).

Pseudomonas aeruginosa, like *S.* Typhimurium, is a T3SS^{+} flagellated pathogen that was previously shown to activate NLRC4 (Sutterwala et al., 2007). ExoU is a T3SS-translocated phospholipase that kills cells independently of NLRC4. Upon infection of BMMs with an ExoU-deficient strain of *P. aeruginosa*, only *Nlrc4*$^{-/-}$ and *Naip1-6*$^{\Delta/\Delta}$ cells are significantly protected from cell death (Fig. 3 C). These results indicate that multiple NAIPs are involved in sensing *P. aeruginosa* T3SS components and flagellin, similar to what we observed with *S.* Typhimurium infection.

Naip1 is required for detection of T3SS needle protein in vivo

In the aforementioned infection experiments, it was not possible to address the role of *Naips* in response to individual bacterial ligands because cytosolic delivery of ligands requires a functional T3SS system, which itself requires simultaneous expression of both the T3SS inner rod and needle proteins. The retroviral lethality assay can be used to express individual bacterial proteins in BMM, but not to address the function of *Naips* in vivo. Thus, to address whether *Naips* are required for NLRC4 activation in response to specific bacterial ligands in vivo, we used a previously described system in which bacterial ligands are fused to the N-terminal domain of anthrax lethal factor (LFn). The LFn domain acts as a signal sequence that targets proteins for cytoso-

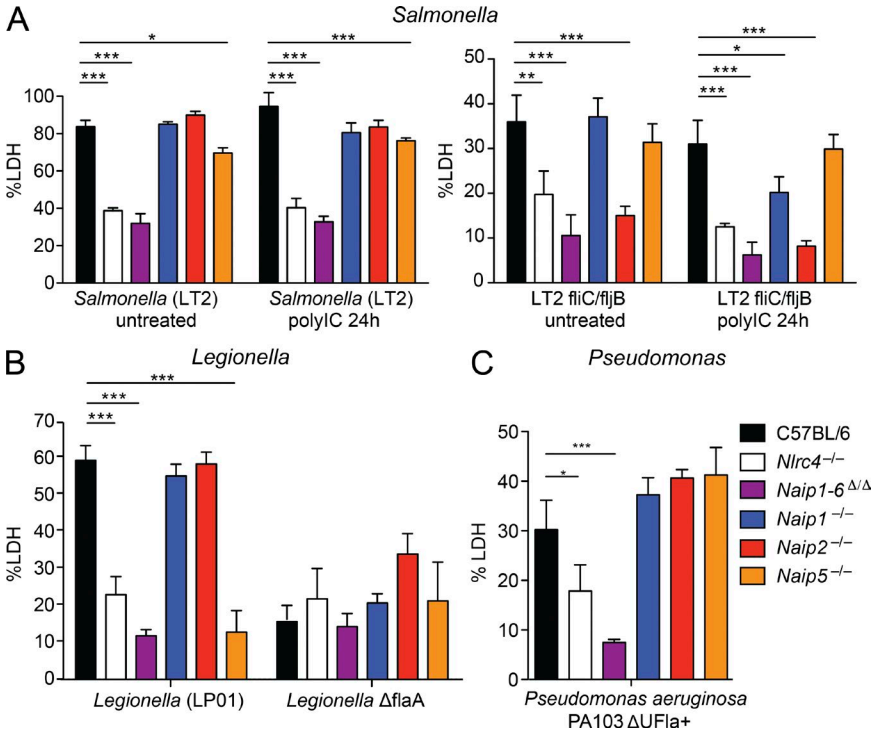

Figure 3. **Requirement for individual NAIPs for pyroptosis during macrophage infection.** (A–C) LDH release assay of supernatants of WT, *Nlrc4*$^{-/-}$, *Naip1-6*$^{\Delta/\Delta}$, *Naip1*$^{-/-}$, *Naip2*$^{-/-}$, and *Naip5*$^{-/-}$ BMMs infected with WT LT2 or flagellin-deficient (*fliC fljB*) *S.* Typhimurium (MOI = 5) for 6 h, with or without 5 µg/ml polyIC 24 h before infection (note different y-axis scales for WT and flagellin-deficient data; A), WT LP02 or flagellin-deficient *L. pneumophila* (MOI = 5) for 4 h (B), or *P. aeruginosa* (MOI = 20) PA103ΔU Fla^{+} for 2 h after 3-h pretreatment with 50 ng/ml LPS (C). Data are representative of two independent experiments (n = 3), mean ± SD; one-way ANOVA, Dunnett's post test: *, P < 0.05; **, P < 0.01; ***, P < 0.001.

lic translocation via the co-administered protective antigen (PA) channel protein (Ballard et al., 1996; Kofoed and Vance, 2011; Zhao et al., 2011). Neither PA nor LFn fusion proteins used individually activate NLRC4, whereas the combination of PA and LFn-flagellin or LFn-rod protein are potent NLRC4 activators (Kofoed and Vance, 2011; Zhao et al., 2011; von Moltke et al., 2012). We previously found that recombinant PA or LFn fusion proteins purified from bacteria were unavoidably contaminated with LPS, which affects the in vivo inflammasome response (von Moltke et al., 2012). Therefore, to reduce the levels of bacterial contaminants as much as possible, we expressed and purified PA and LFn fusions from insect cells. Consistent with endotoxin contamination not playing a role, MyD88/Trif-deficient mice responded to NeedleTox and RodTox as robustly as WT mice (not depicted).

We first used the LFn-PA system to deliver the T3SS system needle protein from *B. thailandensis* into BMMs pretreated with polyIC to induce *Naip1* expression. As expected, we found that WT, *Naip2*$^{-/-}$, or *Naip5*$^{-/-}$ cells released LDH, whereas *Nlrc4*$^{-/-}$, *Naip1*$^{-/-}$, and *Naip1-6*$^{\Delta/\Delta}$ BMMs were fully protected from pyroptosis (Fig. 4 A). To determine which NAIPs are responsible for detection of T3SS needle protein in vivo, we treated mice with NeedleTox intravenously. Resident peritoneal macrophages, a major contributor to FlaTox-induced pathology (von Moltke et al., 2012), express robust levels of *Naip1* and *Naip2* (Rayamajhi et al., 2013). Furthermore, *Naip1*, *2*, *5*, and *6* are expressed at high levels in the spleen and small and large intestine (Rayamajhi et al., 2013; Sellin et al., 2014; Allam et al., 2015). Indeed, similar to treatment with FlaTox (von Moltke et al., 2012), WT mice treated with NeedleTox exhibited a drastic loss of body temperature (Fig. 4 B) accompanied by a highly significant increase in hematocrit (%RBC volume of blood; Fig. 4 C). *Naip2*$^{-/-}$ or *Naip5*$^{-/-}$ mice showed the same pathological response as WT animals, whereas *Nlrc4*$^{-/-}$, *Naip1*$^{-/-}$, and *Naip1-6*$^{\Delta/\Delta}$ mice were completely protected from NeedleTox. These data show that systemic activation of the NAIP1/NLRC4 inflammasome produces rapid pathology and that NAIP1 is specifically required for detection of T3SS needle protein in vivo.

Naip2 is required for detection of T3SS inner rod protein in vivo

We fused LFn to the inner rod protein (PrgJ) from the *S.* Typhimurium SPI-1 T3SS and combined the resulting LFn-rod fusion protein with recombinant PA (both purified from insect cells) to generate "RodTox." Upon treatment of BMMs with RodTox, WT, *Naip1*$^{-/-}$, and *Naip5*$^{-/-}$ BMM underwent pyroptosis, whereas *Nlrc4*$^{-/-}$, *Naip1-6*$^{\Delta/\Delta}$, and *Naip2*$^{-/-}$ BMMs were significantly protected from cell death (Fig. 4 D). Upon intravenous delivery of RodTox, WT, *Naip1*$^{-/-}$, and *Naip5*$^{-/-}$ animals exhibited a rapid hypothermic response and hematocrit increase, whereas *Nlrc4*$^{-/-}$, *Naip1-6*$^{\Delta/\Delta}$, and *Naip2*$^{-/-}$ animals were completely protected (Fig. 4, E and F). These results demonstrate that NAIP2 is required for NLRC4 inflammasome activation in response to T3SS rod protein in vivo.

Naip1 and *Naip2* are dispensable for detection of flagellin in vivo

We expressed a fusion of LFn to *L. pneumophila* flagellin in insect cells and combined the fusion protein with PA to generate

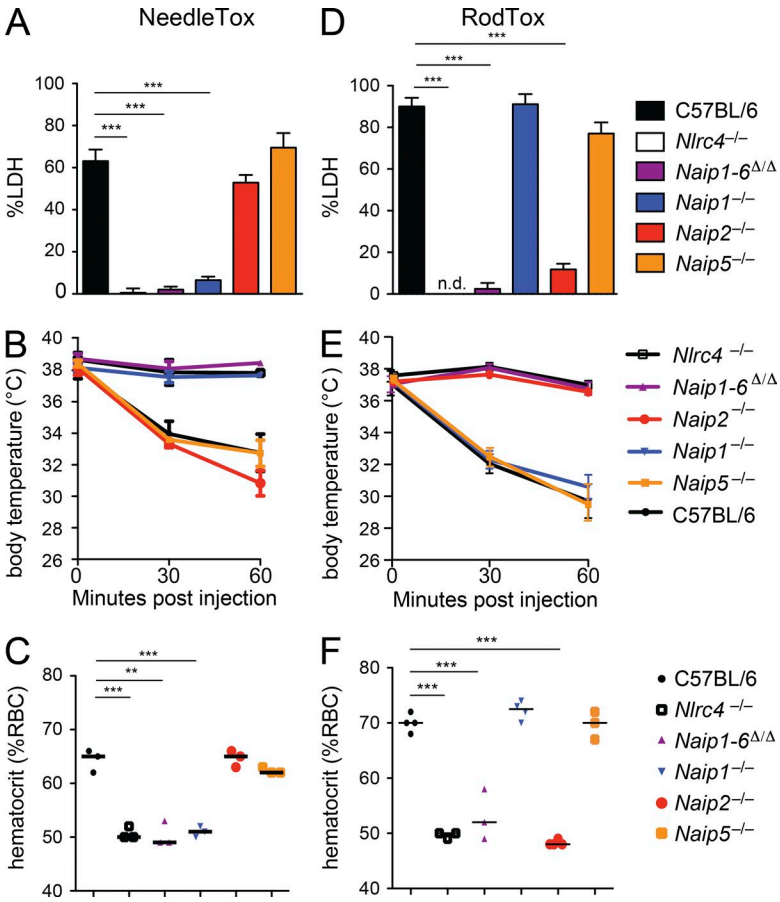

Figure 4. **NAIP1 and NAIP2 detect T3SS needle and rod protein, respectively.** (A) LDH release assay of WT, *Nlrc4*$^{-/-}$, *Naip1-6*$^{\Delta/\Delta}$, *Naip1*$^{-/-}$, *Naip2*$^{-/-}$, and *Naip5*$^{-/-}$ BMMs treated with 4 µg/ml PA and 200 ng/ml LFn-needle for 4 h after 24-h pretreatment with 5 µg/ml polyIC. (B) Rectal temperatures of WT, *Nlrc4*$^{-/-}$, *Naip1-6*$^{\Delta/\Delta}$, *Naip1*$^{-/-}$, *Naip2*$^{-/-}$, and *Naip5*$^{-/-}$ mice injected with 0.8 µg/g body weight of PA and 80 ng/g LFn-needle intravenously (retroorbitally). (C) As in B, except hematocrit was measured at 60 min after injection. (D) As in A, except BMMs were treated with 4 µg/ml PA and 10 ng/ml LFn-rod for 4 h. n.d., not detectable. (E) As in B, except mice were injected with 0.8 µg/g body weight of PA and 1 ng/g LFn-rod intravenously (retroorbitally). (F) As in E, except hematocrit was measured at 60 min after injection. (C and F) Horizontal lines indicate median. Data are representative of two independent experiments (n = 3), mean ± SD; one-way ANOVA, Dunnett's post test: **, P < 0.01; ***, P < 0.001.

FlaTox. Upon treatment of BMM with FlaTox, we observed that WT, *Naip2*$^{-/-}$, and *Naip1*$^{-/-}$ cells all underwent comparable levels of pyroptosis, whereas *Naip5*$^{-/-}$ macrophages were partially, but significantly, protected (Fig. 5 A). In contrast, *Nlrc4*$^{-/-}$ and *Naip1-6*$^{\Delta/\Delta}$ cells were fully protected from FlaTox. These results demonstrate that NAIP1 and NAIP2 are not required for NLRC4 activation in response to flagellin and suggest the involvement of an NAIP protein other than NAIP5 in the detection of flagellin. This NAIP gene is most likely to be NAIP6 based on previous biochemical experiments and its high degree of sequence identity to NAIP5 (Kofoed and Vance, 2011; Zhao et al., 2011; Tenthorey et al., 2014).

Comparable with our in vitro results, *Nlrc4*$^{-/-}$ and *Naip1-6*$^{\Delta/\Delta}$ mice were fully protected from intravenous FlaTox treatment (Fig. 5, B–D). As previously observed, *Naip5*$^{-/-}$ mice showed a delayed loss of body temperature and a slight, but statistically significant increase in hematocrit compared with WT animals after 30 min (Fig. 5, B and C; von Moltke et al., 2012). At 90 min, when WT, *Naip2*$^{-/-}$, and *Naip1*$^{-/-}$ animals had already succumbed to FlaTox, *Naip5*$^{-/-}$ exhibited a marked increase in hematocrit compared with *Nlrc4*$^{-/-}$ and *Naip1-6*$^{\Delta/\Delta}$ mice. Thus, NAIP5 and at least one other NAIP (likely NAIP6) are responsive to flagellin in vivo, whereas NAIP1 and NAIP2 are not required for NLRC4 activation in response to flagellin in vivo.

Collectively, our results provide unequivocal evidence for an essential role of NAIP proteins in NLRC4 inflammasome activation in response to specific bacterial ligands in vivo. In particular, we find that NAIP1 is required for T3SS needle detection, NAIP2 is required for T3SS inner rod detection, and NAIP5 participates in flagellin detection (most likely in conjunction with NAIP6). Our results provide genetic evidence that is entirely consistent with extensive prior biochemical and structural data. NLRC4 has previously been suggested also to require phosphorylation for its activation (Qu et al., 2012). Our data do not address this requirement, but do strongly imply that phosphorylation cannot circumvent the requirement for NAIPs in NLRC4 activation in response to bacterial ligands, consistent with previous conclusions (Matusiak et al., 2015). Lastly, our results illustrate the power of CRISPR/Cas9 to dissect genetically a highly repetitive gene cluster that had previously been technically difficult to target using conventional methodologies.

MATERIALS AND METHODS

Mouse experiments. All mice were specific pathogen free, maintained under a 12-h light–dark cycle (7 a.m. to 7 p.m.), and given a standard chow diet (Harlan irradiated laboratory animal diet) ad libitum. *Naip5*$^{-/-}$ mice on the B6 back-

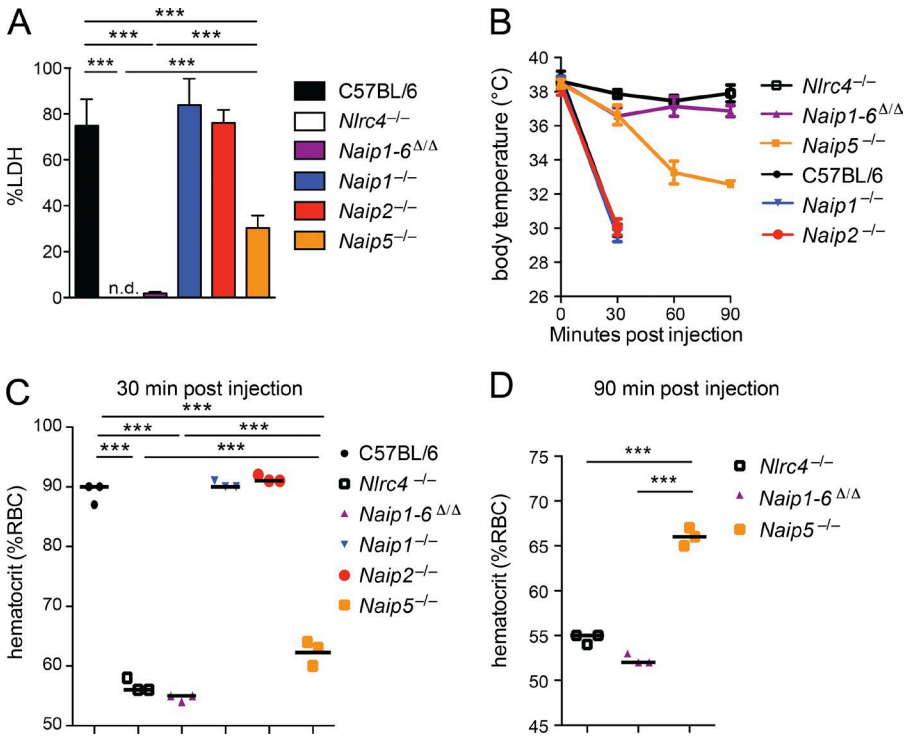

Figure 5. **NAIP specifically senses flagellin protein in vitro and in vivo.** (A) LDH release assay of WT, *Nlrc4*$^{-/-}$, *Naip1-6*$^{\Delta/\Delta}$, *Naip1*$^{-/-}$, *Naip2*$^{-/-}$, and *Naip5*$^{-/-}$ BMMs treated with 4 µg/ml PA and 4 µg/ml LFn-flagellin for 4 h. n.d., not detectable. (B) Rectal temperatures of WT, *Nlrc4*$^{-/-}$, *Naip1-6*$^{\Delta/\Delta}$, *Naip1*$^{-/-}$, *Naip2*$^{-/-}$, and *Naip5*$^{-/-}$ mice injected with 0.8 µg/g body weight of PA and 0.8 µg/g LFn-flagellin intravenously (retroorbitally). (C) As in B, except hematocrit was measured at 30 min after injection. (D) As in B, except hematocrit was measured at 90 min after injection. At this time point, WT, *Naip1*$^{-/-}$, and *Naip2*$^{-/-}$ mice had already succumbed to the treatment. (C and D) Horizontal lines indicate median. Data are representative of two independent experiments (n = 3), mean ± SD; one-way ANOVA, Dunnett's post test: ***, P < 0.001.

ground were described previously (Lightfield et al., 2008). WT C57BL/6J mice were originally obtained from The Jackson Laboratory, and *Nlrc4*$^{-/-}$ animals were from V. Dixit (Genentech, South San Francisco, CA; Mariathasan et al., 2004). CRISPR/Cas9 targeting was performed by pronuclear injection of Cas9 mRNA and sgRNA into fertilized zygotes from colony-born C57BL/6J mice, essentially as described previously (Wang et al., 2013). Founder mice were genotyped as described in Genotyping of *Naip* alleles, and founders carrying *Naip* mutations were bred one generation to C57BL/6J to separate modified *Naip* haplotypes. Homozygous lines were generated by interbreeding heterozygotes carrying matched *Naip* haplotypes. All animal experiments complied with the regulatory standards of, and were approved by, the University of California, Berkeley Institutional Animal Care and Use Committee.

Genotyping of *Naip* alleles. Exon 6 and the surrounding intronic regions were amplified by PCR using the following primers (all 5′ to 3′): Naip1 fwd, TCCTGCAGCTGAGCA TCTA; and rev, CAAGTGCCTATAACTCCACCAT; Naip2 fwd, AACTGCATAAAATCCCCCAAAT; and rev, AGA GACAGAGACACAGAGAAC; Naip3 fwd, TGTTTGGAA CTGCATAAAAATCCT; and rev, AGACAGAGACACAGA AGAACA; Naip5 fwd, GCCCCAGATCCCCTCTCT GTGT; and rev, GAGGACAGCGATTTAGTACAGT; and Naip6 fwd, TGAAGACAGGTACAGTGTGTG; and rev, GTGGATGGAGTAGAAAGTGGG. All primers distinguish the specific *Naip* paralogues. Primers were used at 200 nM in a reaction with 2.5 mM $MgCl_2$ and 75 µM dNTPs and 1 U Taq polymerase (Thermo Fisher Scientific) per reaction. Cleaned PCR products were diluted 1:16 and sequenced using Sanger sequencing (Berkeley DNA Sequencing facility).

Retroviral constructs and production. Genes encoding *L. pneumophila* flagellin (FlaA; accession YP_095369), *S.* Typhimurium T3SS inner rod protein (PrgJ, accession NP_461793), and *B. thailandensis* T3SS needle protein (BTH_RS04290; accession WP_009896110) were cloned into a replication-defective mouse stem cell retroviral construct (pMSCV2.2). Retroviral particles were generated with GP2-293 packaging cells and were used to transduce BM cells after 48 and 72 h of culture in macrophage colony-stimulating factor. Cells were analyzed 4 d after the first transduction.

Toxins. Recombinant proteins (PA, LFn-flagellin, LFn-needle, and LFn-rod) were purified from insect cells. His_6-LFn fused to the N terminus of the indicated gene (Ser-Thr-Arg linker) or His_6-PA was cloned into pFastBac Dual (Invitrogen) using the SalI and NotI restriction sites. Recombinant bacmids were generated to infect Sf9 cells according to the manufacturer's instruction (pFastBac Dual; Invitrogen). After 72 h of infection with P2 baculovirus, insect cells were lysed with buffered detergent (1% NP-40 in 20 mM Tris and 150 mM NaCl, pH 8.0) and then clarified by centrifugation at 50,000 *g* for 45 min at 4°C. Proteins were purified using Ni-NTA agarose (QIAGEN), eluted with 500 mM imidazole in 20 mM Tris and 500 mM NaCl, pH 8.0, and then dialyzed into 20 mM Tris, pH 8.0, and subjected to anion exchange chromatography (ENrich Q column; Bio-Rad Laboratories)

using a gradient elution into high-salt buffer (20 mM Tris and 1 M NaCl, pH 8.0). Fractions containing protein were concentrated using Amicon-Ultra centrifugal filters (EMD Millipore) and quantified using a BCA kit (Thermo Fisher Scientific). Endotoxin contamination of the preparations (determined using a LAL chromogenic endotoxin quantitation kit;Thermo Fisher Scientific) was estimated to result in application of ∼0.2 ng/mouse (Needle and RodTox) or 0.4 ng/mouse (FlaTox) of endotoxin, an amount below the threshold for systemic responses in mice (Copeland et al., 2005).

Toxin doses were 0.8 µg/g body weight of PA combined with 0.8 µg/g LFn-Fla, 80 ng/g LFn-needle, or 1 ng/g LFn-rod for intravenous (retroorbital) delivery or 4 µg/ml PA combined with 4 µg/ml LFn-flagellin, 200 ng/ml LFn-needle, or 10 ng/ml LFn-rod for in vitro delivery. Rectal temperature was determined using a MicroTherma 2T thermometer (Braintree Scientific). Blood for hematocrit was collected by retroorbital bleed into StatSpin microhematocrit tubes (Thermo Fisher Scientific).

Macrophages. BM was harvested from mouse femurs, and cells were differentiated into macrophages by culture in RPMI supplemented with L929 cell supernatant and 10% fetal bovine serum (20% for *P. aeruginosa* experiments) in a humidified incubator (37°C, 5% CO_2). Cells were primed with 5 µg/ml polyIC for 24 h before *S.* Typhimurium infection or LFn-needle/PA treatment and with 50 ng LPS 3 h before *P. aeruginosa* infection.

Bacterial strains. *L. pneumophila* strains LP02 and LP02Δ*flaA* have been described previously (Ren et al., 2006). *S.* Typhimurium strain LT2 and the flagellin-deficient mutant were gifts from A.Van der Velden and M. Starnbach (Harvard Medical School, Boston, MA). *S.* Typhimurium was grown overnight in Luria-Bertani broth and was then reinoculated at a dilution of 1:40 and grown at 37°C to mid-exponential phase (3 h) to induce expression of the *Salmonella* pathogenicity island 1 T3SS. *P. aeruginosa* PA103ΔU Fla^+ (Jain and Kazmierczak, 2014), an isogenic strain of PA103ΔU, a T3SS-positive, naturally aflagellate laboratory strain (Liu, 1966), was freshly streaked to VBM agar from −80°C glycerol stocks before each experiment. Single colonies were used to inoculate 3 ml Lysogeny broth (LB) overnight cultures (37°C, 225 rpm). Overnight cultures were diluted 1:100 into 3 ml LB, grown at 37°C with shaking to an OD_{600} of ∼0.2–0.3. Bacteria were washed in PBS.

Cytotoxicity assays. Cytotoxicity was measured by evaluation of the activity of LDH released from macrophages (Lightfield et al., 2008). Overnight cultures of *L. pneumophila* in stationary phase or $SPI1^+$ *S.* Typhimurium were added at an MOI of 5 to a 96-well plate containing 5×10^4 macrophages per well. *P. aeruginosa* was used at an MOI of 20 in 24-well plates at 2×10^5 macrophages/well. Plates were spun for 10 min at 250 *g* for similar infectivity of motile and nonmotile strains. For *S.* Typhimurium, 20 µg/ml gentamicin was added 30 min after infection to kill extracellular bacteria. Culture supernatants were assayed for LDH activity after 2 (*P. aeruginosa*), 4 (*L. pneumophila*), or 6 h (*S.* Typhimurium). Note that LT2 is a highly passaged *S.* Typhimurium strain with low SPI1 expression, therefore necessitating analysis at a relatively late time point. Infection-specific lysis was calculated as the percentage of detergent-lysed macrophages.

ACKNOWLEDGMENTS

We acknowledge the assistance of the University of California, Berkeley Cancer Research Laboratory Flow Cytometry Laboratory, Eric Chen and Peter Dietzen for technical support, and the Vance and Barton Labs for discussions.

This work was supported by National Institutes of Health (NIH) grants to R.E. Vance (AI075039 and AI063302). R.E. Vance is a Burroughs Wellcome Fund Investigator in the Pathogenesis of Infectious Disease and an Investigator of the Howard Hughes Medical Institute. B.I. Kazmierczak is supported by an NIH grant (AI081825) and I. Rauch by the Austrian Science Fund (FWF; the Erwin Schrödinger Fellowship J3789-B22).

The authors declare no competing financial interests.

Submitted: 17 November 2015

Accepted: 16 March 2016

REFERENCES

Allam, R., M.H. Maillard, A. Tardivel, V. Chennupati, H. Bega, C.W. Yu, D. Velin, P. Schneider, and K.M. Maslowski. 2015. Epithelial NAIPs protect against colonic tumorigenesis. *J. Exp. Med.* 212:369–383. http://dx.doi.org/10.1084/jem.20140474

Ballard, J.D., R.J. Collier, and M.N. Starnbach. 1996. Anthrax toxin-mediated delivery of a cytotoxic T-cell epitope in vivo. *Proc. Natl. Acad. Sci. USA.* 93:12531–12534. http://dx.doi.org/10.1073/pnas.93.22.12531

Copeland, S., H.S. Warren, S.F. Lowry, S.E. Calvano, and D. Remick. Inflammation and the Host Response to Injury Investigators. 2005. Acute inflammatory response to endotoxin in mice and humans. *Clin. Diagn. Lab. Immunol.* 12:60–67.

Diez, E., S.-H. Lee, S. Gauthier, Z. Yaraghi, M. Tremblay, S. Vidal, and P. Gros. 2003. *Birc1e* is the gene within the *Lgn1* locus associated with resistance to *Legionella pneumophila*. *Nat. Genet.* 33:55–60. http://dx.doi.org/10.1038/ng1065

Growney, J.D., and W.F. Dietrich. 2000. High-resolution genetic and physical map of the Lgn1 interval in C57BL/6J implicates Naip2 or Naip5 in *Legionella pneumophila* pathogenesis. *Genome Res.* 10:1158–1171. http://dx.doi.org/10.1101/gr.10.8.1158

Hu, Z., Q. Zhou, C. Zhang, S. Fan, W. Cheng, Y. Zhao, F. Shao, H.-W. Wang, S.-F. Sui, and J. Chai. 2015. Structural and biochemical basis for induced self-propagation of NLRC4. *Science.* 350:399–404. http://dx.doi.org/10.1126/science.aac5489

Jain, R., and B.I. Kazmierczak. 2014. A conservative amino acid mutation in the master regulator FleQ renders *Pseudomonas aeruginosa* aflagellate. *PLoS One.* 9:e97439. http://dx.doi.org/10.1371/journal.pone.0097439

Kofoed, E.M., and R.E. Vance. 2011. Innate immune recognition of bacterial ligands by NAIPs determines inflammasome specificity. *Nature.* 477:592–595. http://dx.doi.org/10.1038/nature10394

Kortmann, J., S.W. Brubaker, and D.M. Monack. 2015. Cutting edge: Inflammasome activation in primary human macrophages is dependent on flagellin. *J. Immunol.* 195:815–819. http://dx.doi.org/10.4049/jimmunol.1403100

Lamkanfi, M., and V.M. Dixit. 2014. Mechanisms and functions of inflammasomes. *Cell.* 157:1013–1022. http://dx.doi.org/10.1016/j.cell.2014.04.007

Lightfield, K.L., J. Persson, S.W. Brubaker, C.E. Witte, J. von Moltke, E.A. Dunipace, T. Henry, Y.-H. Sun, D. Cado, W.F. Dietrich, et al. 2008. Critical function for Naip5 in inflammasome activation by a conserved carboxy-terminal domain of flagellin. *Nat. Immunol.* 9:1171–1178. http://dx.doi.org/10.1038/ni.1646

Lightfield, K.L., J. Persson, N.J. Trinidad, S.W. Brubaker, E.M. Kofoed, J.-D. Sauer, E.A. Dunipace, S.E. Warren, E.A. Miao, and R.E. Vance. 2011. Differential requirements for NAIP5 in activation of the NLRC4 inflammasome. *Infect. Immun.* 79:1606–1614. http://dx.doi.org/10.1128/IAI.01187-10

Liu, P.V. 1966. The roles of various fractions of *Pseudomonas aeruginosa* in its pathogenesis. 3. Identity of the lethal toxins produced in vitro and in vivo. *J. Infect. Dis.* 116:481–489. http://dx.doi.org/10.1093/infdis/116.4.481

Mariathasan, S., K. Newton, D.M. Monack, D. Vucic, D.M. French, W.P. Lee, M. Roose-Girma, S. Erickson, and V.M. Dixit. 2004. Differential activation of the inflammasome by caspase-1 adaptors ASC and Ipaf. *Nature.* 430:213–218. http://dx.doi.org/10.1038/nature02664

Matusiak, M., N. Van Opdenbosch, L. Vande Walle, J.-C. Sirard, T.-D. Kanneganti, and M. Lamkanfi. 2015. Flagellin-induced NLRC4 phosphorylation primes the inflammasome for activation by NAIP5. *Proc. Natl. Acad. Sci. USA.* 112:1541–1546. http://dx.doi.org/10.1073/pnas.1417945112

Molofsky, A.B., B.G. Byrne, N.N. Whitfield, C.A. Madigan, E.T. Fuse, K. Tateda, and M.S. Swanson. 2006. Cytosolic recognition of flagellin by mouse macrophages restricts *Legionella pneumophila* infection. *J. Exp. Med.* 203:1093–1104. http://dx.doi.org/10.1084/jem.20051659

Qu, Y., S. Misaghi, A. Izrael-Tomasevic, K. Newton, L.L. Gilmour, M. Lamkanfi, S. Louie, N. Kayagaki, J. Liu, L. Kömüves, et al. 2012. Phosphorylation of NLRC4 is critical for inflammasome activation. *Nature.* 490:539–542. http://dx.doi.org/10.1038/nature11429

Rayamajhi, M., D.E. Zak, J. Chavarria-Smith, R.E. Vance, and E.A. Miao. 2013. Cutting edge: Mouse NAIP1 detects the type III secretion system needle protein. *J. Immunol.* 191:3986–3989. http://dx.doi.org/10.4049/jimmunol.1301549

Ren, T., D.S. Zamboni, C.R. Roy, W.F. Dietrich, and R.E. Vance. 2006. Flagellin-deficient Legionella mutants evade caspase-1- and Naip5-mediated macrophage immunity. *PLoS Pathog.* 2:e18. http://dx.doi.org/10.1371/journal.ppat.0020018

Sellin, M.E., A.A. Müller, B. Felmy, T. Dolowschiak, M. Diard, A. Tardivel, K.M. Maslowski, and W.-D. Hardt. 2014. Epithelium-intrinsic NAIP/NLRC4 inflammasome drives infected enterocyte expulsion to restrict *Salmonella* replication in the intestinal mucosa. *Cell Host Microbe.* 16:237–248. http://dx.doi.org/10.1016/j.chom.2014.07.001

Sutterwala, F.S., L.A. Mijares, L. Li, Y. Ogura, B.I. Kazmierczak, and R.A. Flavell. 2007. Immune recognition of *Pseudomonas aeruginosa* mediated by the IPAF/NLRC4 inflammasome. *J. Exp. Med.* 204:3235–3245. http://dx.doi.org/10.1084/jem.20071239

Suzuki, S., L. Franchi, Y. He, R. Muñoz-Planillo, H. Mimuro, T. Suzuki, C. Sasakawa, and G. Núñez. 2014. Shigella type III secretion protein MxiI is recognized by Naip2 to induce Nlrc4 inflammasome activation independently of Pkcδ. *PLoS Pathog.* 10:e1003926. http://dx.doi.org/10.1371/journal.ppat.1003926

Tenthorey, J.L., E.M. Kofoed, M.D. Daugherty, H.S. Malik, and R.E. Vance. 2014. Molecular basis for specific recognition of bacterial ligands by NAIP/NLRC4 inflammasomes. *Mol. Cell.* 54:17–29. http://dx.doi.org/10.1016/j.molcel.2014.02.018

von Moltke, J., N.J. Trinidad, M. Moayeri, A.F. Kintzer, S.B. Wang, N. van Rooijen, C.R. Brown, B.A. Krantz, S.H. Leppla, K. Gronert, and R.E. Vance. 2012. Rapid induction of inflammatory lipid mediators by the inflammasome in vivo. *Nature.* 490:107–111. http://dx.doi.org/10.1038/nature11351

von Moltke, J., J.S. Ayres, E.M. Kofoed, J. Chavarría-Smith, and R.E. Vance. 2013. Recognition of bacteria by inflammasomes. *Annu. Rev. Immunol.* 31:73–106. http://dx.doi.org/10.1146/annurev-immunol-032712-095944

Wang, H., H. Yang, C.S. Shivalila, M.M. Dawlaty, A.W. Cheng, F. Zhang, and R. Jaenisch. 2013. One-step generation of mice carrying mutations in multiple genes by CRISPR/Cas-mediated genome engineering. *Cell.* 153:910–918. http://dx.doi.org/10.1016/j.cell.2013.04.025

Wright, E.K., S.A. Goodart, J.D. Growney, V. Hadinoto, M.G. Endrizzi, E.M. Long, K. Sadigh, A.L. Abney, I. Bernstein-Hanley, and W.F. Dietrich. 2003. Naip5 affects host susceptibility to the intracellular pathogen *Legionella pneumophila*. *Curr. Biol.* 13:27–36. http://dx.doi.org/10.1016/S0960-9822(02)01359-3

Yang, J., Y. Zhao, J. Shi, and F. Shao. 2013. Human NAIP and mouse NAIP1 recognize bacterial type III secretion needle protein for inflammasome activation. *Proc. Natl. Acad. Sci. USA.* 110:14408–14413. http://dx.doi.org/10.1073/pnas.1306376110

Zhang, L., S. Chen, J. Ruan, J. Wu, A.B. Tong, Q. Yin, Y. Li, L. David, A. Lu, W.L. Wang, et al. 2015. Cryo-EM structure of the activated NAIP2-NLRC4 inflammasome reveals nucleated polymerization. *Science.* 350:404–409. http://dx.doi.org/10.1126/science.aac5789

Zhao, Y., J. Yang, J. Shi, Y.-N. Gong, Q. Lu, H. Xu, L. Liu, and F. Shao. 2011. The NLRC4 inflammasome receptors for bacterial flagellin and type III secretion apparatus. *Nature.* 477:596–600. http://dx.doi.org/10.1038/nature10510